International Journal of Dynamics and Control
https://doi.org/10.1007/s40435-022-00938-0

Unrestricted horizon predictive control applied to a nonlinear SISO system

Luís A. M. de Castro[1] · **Antonio da S. Silveira**[1] · **Rejane de B. Araújo**[2]

Received: 29 November 2021 / Revised: 1 March 2022 / Accepted: 2 March 2022

Abstract
This paper presents the mathematical formalism, design and evaluation of a minimum order unrestricted horizon predictive control (UHPC) predictive applied to nonlinear chemical process. The UHPC design method is still quite new and this paper contributes further by evaluating its application in a nonlinear system and its robustness properties. The control design is done to ensure stability, robustness, reference tracking and disturbance rejection even in the presence of modeling errors and noise. The evaluation is conducted through numerical simulations for step references and load disturbances with one single system: the continuous stirred tank reactor (CSTR). The UHPC problem are assessed under an incremental control scheme and based on the identified stochastic linear model. The temporal and frequency results of the UHPC are compared to the results of the generalized predictive control (GPC) using the same output prediction horizon. Both controllers are able to eliminate the offset, however the UHPC has greater margins of stability and noise attenuation, being able to maintain the same loop response throughout the control system's operating range, without degrading the performance of the controller, which is not the case with GPC.

Keywords Predictive control · Stochastic control · Kalman predictor · Chemical processes · Nonlinear systems · Robustness analysis

1 Introduction

The research of model-based predictive control (MBPC) started in the early 1970s, where several methods of predictive design have been proposed over the years [1]. One of the first proposals was the minimum variance (MV) regulator presented by [2]. The control objective was to regulate the output signal of the system in relation to a constant reference signal, so that the variance in the output signal, caused by the presence of noise, was minimal.

The MV regulator has a relevant role as a precursor in the development of other model-based predictive control strategies, which today are successfully applied in academia and industry, such as the generalized minimum variance (GMV) control presented by [3] and the generalized predictive control (GPC) method proposed by [4]. Such controllers, GMV and GPC, can be understood as generalizations of the control strategy of the MV regulator, where both are based on a very solid theoretical basis [5].

GPC can be considered the successor to GMV, since the GMV control plus the dynamic matrix control (DMC) presented by [6] led [4] to the GPC synthesis. Even though it is a stochastic MBPC algorithm like GMV, GPC is rarely applied because of its stochastic properties and the noise model is commonly simplified, which leads to the use of the CAR (controlled auto-regressive) model. Not even [7], when presenting the properties of GPC, considered the usage of CARMA (controlled auto-regressive moving average) model in their examples.

GMV and GPC can be represented via a polynomial structure with two degrees of freedom and interacting with all signals involved in a classic control loop. Such a configura-

✉ Luís A. M. de Castro
luismesquita@ufpa.br; luis.mesquita.castro@gmail.com

Antonio da S. Silveira
asilveira@ufpa.br

Rejane de B. Araújo
rejane.barros@ifpa.edu.br

[1] Laboratory of Control and Systems, Federal University of Pará, 66075-110 Belém, PA, Brazil

[2] Department of Control and Industrial Processes, Federal Institute of Pará, 66093-020 Belém, PA, Brazil

Published online: 10 May 2022

tion is known in the literature as canonical RST topology, where three polynomials in the discrete domain represent filters that weight the control, output and reference signals in a control system.

As explained in [8,9], the RST structure facilitates the understanding and implementation of such control techniques, in addition to having wide acceptance in the academic and industrial environment, also allowing the analysis of performance and robustness via methods established within the analysis of control systems and theory, such as frequency domain analysis using the Bode diagram and Nyquist diagram. That said, the controller proposed in this work has its control law implemented in a polynomial way, according to the results to be presented in the next sections.

In the original research by [3], the GMV control law is obtained by minimizing a cost function associated with the concept of generalized systems. The objective is to add in the controller design some parameters that allow to satisfy the characteristics desired by the designer, giving the control loop greater flexibility. The generalized system is defined by the designer and varies according to the parameters to be included in the controller's equation, with the system model to be adopted and with the structure of the cost function to be minimized.

In turn, the GPC presented by [4] is from the extended horizon controller family and generally uses an incremental model of the system to obtain the control signal, calculated by minimizing a cost function similar to the GMV. If the GMV is the simplest and least complex member of the MBPC family, the GPC is the most popular member, being used in numerous segments, encompassing systems of the most different complexities [10].

In terms of mathematical representation of models via polynomial ratio for the synthesis of the GMV and GPC control laws, the literature addresses positional or incremental model for different model structures of the system to be controlled. Generally deterministic models are preferable over stochastic ones, since such a choice facilitates and reduces the design time of predictive controllers, although it is known that such a choice impacts the performance and robustness of the control loop [4,11–13].

Since the consolidation of the predictive control theory, the interest of academia and industry in MBPC controllers has remained high throughout the decades, since applications in several areas present promising results (numerical and experimental), which leverages the study of such control techniques. The strong interest of the scientific and industrial community in predictive control is linked to the ability of these controllers to adequately deal with the various classes of systems found in the real world, for example: stable, unstable, minimum phase, non-minimum phase, linear, nonlinear, integrators, combinations of the above, among others [5,10].

The two representatives of the MBPC family that stand out the most are the GMV and GPC, which are still the object of study for countless researchers in the most varied areas of industrial application, such as: power systems, renewable sources, chemistry, petrochemicals, automobiles, robotics, aerospace, food, telecommunications, air conditioning, civil engineering, among others. That said, the Unrestricted Horizon Predictive Control (UHPC) is a strong candidate to be considered and implemented in such industries in the future where GMV and GPC have wide penetration, since UHPC shares design similarities with both [12,14].

The final UHPC algorithm is the result of constant research to obtain an extended horizon predictive controller based on a stochastic model. Such an approach was avoided, since for both the GMV and GPC algorithm this means an increase in design complexity when the horizon of prediction is extensive or a stochastic model is used instead of a deterministic model, since for both cases it is necessary to solve Diophantine equations. This barrier in the design stage leads many works to use the simplest versions of such controllers, referred to in the literature as GMV and GPC of minimum order, thus limiting the advantages obtained by extending the prediction horizon and by the stochastic approach of the system [14,15].

However, the results presented in [16] raised the interest in further investigation on the extension of the prediction horizon beyond the compensation of time delay in the GMV. In this work, the authors present an entirely new approach to the design of the GMV via the state space, (GMVSS—generalized minimum variance in the state space). The main contribution of the work is the simplicity of design due to the absence of the Diophantine equation in the procedure. The Diophantine equation is solved indirectly and naturally by the problem formulation itself, using the Kalman filter obtained from a stochastic representation in state space. This procedure differs from the original, GMV, via transfer functions, however it provides the same results. Other important works on GMV control via state space are presented in [17,18].

The GMVSS design method is used to overcome the question of solving the Diophantine equation, without increasing the design complexity of the GMV. Based on this premise, [19] presents the first attempt to extend the horizon of prediction beyond the mere compensation of time delay as is done in GMV. Such an algorithm was named as long-range minimum variance (LMV), where the control law obtained is based on a stochastic model. The work investigated how the extension of the prediction horizon affects both the output of the controller and the output of the plant in two classes of systems. The numerical and experimental results presented show that for the same prediction horizon, in terms of control effort, the LMV control is more economical when compared to the classic GPC of [4]. Another advantage of LMV is that it does not use a receding horizon like GPC and other

MBPC algorithms, which reduces the computational burden and complexity of implementing its control law.

However, the observed results did not confirm the expectations regarding the unrestricted extension of the prediction horizon which would guarantee a good result in terms of minimizing damping and variance. On the contrary, by overextending the prediction horizon, as was done in the work, led the control loop to show quite oscillatory behavior [19].

[19] suggested that the problem would be in the synthesis of the controller, since that was a preliminary work and was still under study by the group of researchers. The suspicion was confirmed, the LMV algorithm has a gap, which would be the control prediction horizon. As the LMV is based on GMV and this in turn has only the prediction of the system's output signal, the LMV control inherited this characteristic in its synthesis. The UHPC algorithm is born when the control prediction horizon is included in the controller project, similar to the GPC, filling the gap identified in the LMV synthesis.

In [14] the UHPC based on the GMVSS design method is presented, which has the advantage of the absence of the explicit solution of the Diophantine equation compared to other approaches of the MV type and, for this reason, the prediction horizon can be extended indefinitely, to the unlike other controllers called long-range predictors, where the prediction horizon is usually less than or equal to ten samples. Unlike DMC, GPC and other members of the MBPC family, the UHPC does not use a receding horizon to calculate future control signals. Instead, the two Diophantine equations present in the UHPC synthesis are solved intrinsically using the Kalman filter to obtain the future command signal. In addition to this ease of design, the UHPC is based on stochastic models, being another important difference compared to more common predictive approaches, since considering the noise model that disturbs the system improves the controller's regulation capacity.

The numerical simulations carried out showed that the noise rejection capacity of the UHPC is similar to the MV regulator, but reducing control effort, where the obvious cause for such result is the UHPC extended prediction horizon, which in practice means that the controller "knows" the behavior of future noise in advance, so the controller is able to act in the present in order to reduce the control effort. For example, in the UHPC case the variance of the output variable was 0.2% greater than in the MV case, however the necessary control effort had a 45% smaller variance for the UHPC case in relation to the MV [14].

It is important to note that all numerical simulations reported in [14] were performed with the minimum order UHPC and with a zero weighting factor, which means that all the energy needed to regulate the system output according to the desired reference can be used by the controller and, even with such tuning, the results demonstrated that the control effort required by the UHPC may be feasible to implement in experimental cases.

From the pioneering results, it is evident the need for detailed research with other classes of systems (unstable, non-minimum phase, non-linear) in addition to those already studied, equipped with adequate metrics for the analysis of performance and robustness of the UHPC in its version of minimum order and in its weighted (not minimum) version, in order to investigate how the UHPC tuning impacts the reference tracking and disturbance rejection of the control loop, comparing its results with those of traditional and predictive controllers already consolidated in its theory and applications.

Another inviting aspects to explore in UHPC are the mathematical and structural ways in which the controller presents itself, similar to GMV and GPC, being possible to take advantage of classic methods of analysis of performance and robustness existing in the control literature. In this way, it is possible to propose, justify and validate alternative UHPC design methodologies based on these evaluation criteria. In summary, the UHPC controller appears as a promising option to be explored in the MBPC family.

Based on the previous assumptions, a problem that made (and makes) sense is the investigation of the possibilities offered by the UHPC, so little explored or even unknown by the scientific community, regarding improvements in the minimum variance problem with a synthesis which revolutionizes both performance and design method, surpassing predecessor designs. Table 1 presents some publications, in the last years, using MBPC to deal with offset-free behavior (reference tracking and disturbance rejection) in different areas.

The purpose of this paper is to evaluate in detail the control loop for different tunings of the UHPC applied to the CSTR (continuous stirred tank reactor) chemical process not only to eliminate the steady-state error but also to stabilize nonlinear monovariable systems (to provide an effective closed-loop dynamic). Also comparing aspects of performance, stability and robustness with the classic GPC for handling offset. Particularly, the offset-free tracking is the major goal in the control of industrial processes, where the offset is a result of a variety of causes such as constant reference changes and load disturbances. The choice of this process was motivated, as significant benchmark model, by the fact that it is characterized by a nonlinear behavior, which makes the UHPC design challenging, since the UHPC is still little explored in applications in the control literature, in particular nonlinear systems.

This paper is organized as follows: Sect. 2 presents the mathematical formalism of the UHPC design. Section 3 presents UHPC design using the state space theory. Section 4 discusses some important concepts of the performance and

Table 1 Publications using MBPC

Area	Application
Power systems	Predictive control of a fresnel collector field [20]
Process control	Predictive control of a zinc hydrometallurgy plant [21]
Robotics	Predictive control of a two-wheeled mobile robot [22]
Aerospace	Predictive control of an unmanned aerial vehicle [23]
HVAC systems	Predictive control of ventilation in an air conditioning system [24]

robustness indices found in the control literature. Numerical results for two benchmark chemical processes are presented in Sect. 5. Finally, conclusions are given in Sect. 6.

2 Unrestricted horizon predictive control

Consider a CARMA linear model of a single-input single-output (SISO) system characterized by the following positional discrete equation [2,25]:

$$A(q^{-1})y(k) = q^{-d}B(q^{-1})u(k) + C(q^{-1})\xi(k) \tag{1}$$

where $y(k)$ is the system output, $u(k)$ is the control signal, d is the time delay, $\xi(k)$ is a Gaussian disturbance sequence and q^{-1} is the backward shift operator such that $q^{-n}y(k) = y(k-n)$, respectively. The roots of the polynomials $A(q^{-1})$ and $B(q^{-1})$ are the open-loop poles and zeros of the system. Similarly to the GMV of [3], the UHPC of [14] regards a generalized predicted output N_y steps ahead (with $N_y \geq d$), which is given by

$$\begin{aligned}\hat{\phi}(k+N_y) = {} & P(q^{-1})\hat{y}(k+N_y) \\ & + T(q^{-1})y_r(k+d) - Q(q^{-1})u(k)\end{aligned} \tag{2}$$

and is posed into a stochastic optimization problem. The generalized output proposed by [3] comes directly from the developments in optimal control and since then, minimizing the tracking error and the control effort is common sense in optimal servo control. To simplify the analysis, the generalized predicted output $\hat{\phi}(k+N_y)$ in Eq. (2) is reset to its minimum form, the minimum order UHPC controller has $P(q^{-1}) = T(q^{-1}) = 1$ and $Q(q^{-1}) = \lambda$. The UHPC control law is obtained by minimizing the cost function given by

$$\Upsilon = \Lambda\left[\phi^2\left(k+N_y\right)\right] = \hat{\phi}^2\left(k+N_y\right) \tag{3}$$

where $y_r(k)$ is the nonzero reference signal (setpoint), λ is the control weighting factor, N_y is the output prediction horizon and $\Lambda[\cdot]$ denotes the mathematical expectation operator, respectively. The relative importance of controller performance criteria varies with the application area. For example, in process control it is generally found that energetic control signals are undesirable, a slowly responding loop being preferred, and plant models are poorly specified in terms of dead-time and order as well as their transfer function parameters. Emphasis is therefore placed on robust and consistent performance despite variations in quantities such as dead-time and despite sustained load disturbances [11].

Shifting Eq. (1) N_y steps ahead leads to

$$\begin{aligned}A(q^{-1})y(k+N_y) = {} & B(q^{-1})u(k+N_y-d) \\ & + C(q^{-1})\xi(k+N_y)\end{aligned} \tag{4}$$

Clearly $\xi(k+N_y)$ is unknown, and therefore it can be represented with present and future parts:

$$\frac{C(q^{-1})}{A(q^{-1})}\xi(k+N_y) = \frac{F(q^{-1})}{A(q^{-1})}\xi(k) + E(q^{-1})\xi(k+N_y) \tag{5}$$

whereas its diophantine noise equation is given by

$$C(q^{-1}) = A(q^{-1})E(q^{-1}) + q^{-N_y}F(q^{-1}) \tag{6}$$

where $n_e = N_y - 1$ and $n_f = n_a - 1$; with n_a, n_e and n_f being the order of the polynomials $A(q^{-1})$, $E(q^{-1})$ and $F(q^{-1})$, respectively.

In contrast to GMV of [3], since $N_y \geq d$, the control signal $u(k+N_y-d)$ from Eq. (4) is also unknown. As well as for the stochastic part, it can be represented by present and future parts [14], which does not exist in the GMV control problem:

$$\begin{aligned}\frac{B(q^{-1})}{A(q^{-1})}u(k+N_y-d) = {} & \frac{H(q^{-1})}{A(q^{-1})}u(k) \\ & + J(q^{-1})u(k+N_y-d)\end{aligned} \tag{7}$$

whereas its diophantine command equation is given by

$$B(q^{-1}) = A(q^{-1})J(q^{-1}) + q^{-(N_y-d)}H(q^{-1}) \tag{8}$$

where $n_j = N_y - d - 1$ and $n_h = n_a - 1$; with n_j and n_h being the order of the polynomials $J(q^{-1})$ and $H(q^{-1})$,

respectively.Using only the known data, the predicted output $\hat{y}\left(k+N_y \mid k\right)$ is

$$\hat{y}\left(k+N_y \mid k\right)=\frac{H(q^{-1})}{A(q^{-1})}u\left(k\right)+\frac{F(q^{-1})}{A(q^{-1})}\xi\left(k\right) \tag{9}$$

and so the current stochastic signal $\xi(k)$, calculated from the estimation error, is given by

$$\xi(k)=\frac{y\left(k\right)-q^{-N_y}\hat{y}\left(k+N_y \mid k\right)}{E(q^{-1})}-\frac{q^{-d}J(q^{-1})}{E(q^{-1})}u\left(k\right) \tag{10}$$

Substituting Eq. (10) into Eq. (9) and after some algebric manipulations, the N_y steps ahead minimum variance predictor (MVP) turns to

$$\hat{y}\left(k+N_y \mid k\right)=\frac{E(q^{-1})H(q^{-1})-q^{-d}F(q^{-1})J(q^{-1})}{C(q^{-1})}u(k)+\frac{F(q^{-1})}{C(q^{-1})}y(k) \tag{11}$$

The roots of polynomial $C(q^{-1})$ must be within the unit circle for the MVP to be stable. The minimum order UHPC control law is obtained through the minimization of Eq. (3), resulting in

$$u\left(k\right)=\frac{C(q^{-1})y_r\left(k+d\right)-F(q^{-1})y\left(k\right)}{\lambda C(q^{-1})+E(q^{-1})H(q^{-1})-q^{-d}F(q^{-1})J(q^{-1})} \tag{12}$$

By now, some interesting points are worth to mention:

- The extended horizon N_y is embedded into $H(q^{-1})$;
- If $N_y = d$, UHPC turns to the minimum order GMV presented in [3];
- if $N_y = d$ and $\lambda = 0$, UHPC turns to the MV regulator presented in [2];
- If the plant does not have a natural integrator, its insertion, in order to ensure zero error in steady-state for step inputs, is obtained through the incremental action, $u(k) = u(k-1) + \Delta u(k)$, $\Delta = 1 - q^{-1}$, turning the model in Eq. (1) into a CARIMA (controlled auto-regressive integrated moving-average) model, given by

$$\Delta A(q^{-1})y(k)=q^{-d}B(q^{-1})\Delta u(k)+C(q^{-1})\xi(k) \tag{13}$$

Thus, the control law in Eq. (12) becomes

$$\Delta u\left(k\right)=\frac{C(q^{-1})y_r\left(k+d\right)-F(q^{-1})y\left(k\right)}{\lambda C(q^{-1})+E(q^{-1})H(q^{-1})-q^{-d}F(q^{-1})J(q^{-1})} \tag{14}$$

and the degree of $F(q^{-1})$ and $H(q^{-1})$ changes to n_a;

- The use of weighting filters for $y(k)$, $y_r(k)$, and $u(k)$ or $\Delta u(k)$ in Eq. (2) instead of using only the weighting factor λ is feasible and easy to implement. However, for the sake of simplicity, this approach will not be exploited in the present work.

The term 'unrestricted horizon' refers to the limitation existing in the GMV control where the prediction horizon N_y only compensated for the time delay d, that is, $N_y \leq d$. This limitation is eliminated in the UHPC control, as the prediction horizon can take $N_y \geq d$ values. The big issue in predicting a long ahead horizon is clearly the solution of Eqs. (6) and (8), since the control problem increases due to $n_e = N_y - 1$ and $n_j = N_y - d - 1$. This was one of the reasons why [3] once suggested to keep $d \leq 3$, consequently moving away from the possibility of dealing with high frequency sampling dependent systems, since the sampling period needed to be large in order to keep d as small as possible. In the next section, the GMVSS method is presented for dealing with this issue [16].

3 UHPC in the state space

The mathematical formulation presented in this section differs slightly from [16] due to the consideration of an extended prediction horizon N_y. The formulation presented in [16] differs from the one derived in [3] only in the design procedure, i.e., the control law and closed-loop results are the same.

A CARMA state space linear model is used, where the system in Eq. (1) is rewritten as

$$x\left(k\right)=\mathbf{A}x\left(k-1\right)+\mathbf{B}u\left(k-d\right)+\mathbf{\Gamma}\xi\left(k-1\right) \tag{15}$$

$$y\left(k\right)=\mathbf{C}x\left(k\right)+\xi\left(k\right) \tag{16}$$

Therefore, shifting Eq. (15) N_y steps ahead, the output equation becomes

$$y\left(k+N_y\right)=\mathbf{C}\mathbf{A}^{N_y}x\left(k\right)+\sum_{i=d}^{N_y}\mathbf{C}\mathbf{A}^{N_y-i}\mathbf{B}u\left(k-d+i\right)+\sum_{i=1}^{d-1}\mathbf{C}\mathbf{A}^{N_y-i}\mathbf{B}u\left(k-d+i\right)+\xi\left(k+N_y\right)+\sum_{i=1}^{N_y}\mathbf{C}\mathbf{A}^{N_y-i}\mathbf{\Gamma}\xi\left(k-1+i\right) \tag{17}$$

As in the previous section, the stochastic and control signal parts can be divided into present and future ones

$$\xi\left(k+N_y\right)+\sum_{i=1}^{N_y}\mathbf{C}\mathbf{A}^{N_y-i}\boldsymbol{\Gamma}\xi\left(k-1+i\right)=\underbrace{\mathbf{C}\mathbf{A}^{N_y-1}\boldsymbol{\Gamma}\xi\left(k\right)}_{\text{present}}+\underbrace{\xi\left(k+N_y\right)+\sum_{i=2}^{N_y}\mathbf{C}\mathbf{A}^{N_y-i}\boldsymbol{\Gamma}\xi\left(k-1+i\right)}_{\text{future}}$$

$$\sum_{i=d}^{N_y}\mathbf{C}\mathbf{A}^{N_y-i}\mathbf{B}u\left(k-d+i\right)=\underbrace{\mathbf{C}\mathbf{A}^{N_y-d}\mathbf{B}u\left(k\right)}_{\text{present}}+\underbrace{\sum_{i=d+1}^{N_y}\mathbf{C}\mathbf{A}^{N_y-i}\mathbf{B}u\left(k-d+i\right)}_{\text{future}}$$

Neglecting the future parts and using Eq. (16), the MVP is given by

$$\hat{y}\left(k+N_y\mid k\right)=\left(\mathbf{C}\mathbf{A}^{N_y}-\mathbf{C}\mathbf{F}\mathbf{C}\right)\bar{x}\left(k\right)+\mathbf{C}\mathbf{H}u\left(k\right)+\sum_{i=1}^{d-1}\mathbf{C}\mathbf{A}^{N_y-i}\mathbf{B}u\left(k-d+i\right)+\mathbf{C}\mathbf{F}y\left(k\right)\tag{18}$$

where $\mathbf{F}=\mathbf{A}^{N_y-1}\boldsymbol{\Gamma}$, $\mathbf{H}=\mathbf{A}^{N_y-d}\mathbf{B}$ and $\bar{x}\left(k\right)$ is the Kalman Filter estimated state vector of the CARMA system in (15) and (16), given by

$$\bar{x}\left(k\right)=\left(\mathbf{A}-\boldsymbol{\Gamma}C\right)\bar{x}\left(k-1\right)+\mathbf{B}u\left(k-d\right)+\boldsymbol{\Gamma}y\left(k-1\right)$$

which is equivalent to the one step ahead MVP of [26] and its use is necessary in the practical sense due to the lack of measured information from the states. It is interesting to notice that $\mathbf{F}^T=\left[\begin{array}{cccc}f_0 & f_1 & \cdots & f_{n_a-1}\end{array}\right]$ and $\mathbf{H}^T=\left[\begin{array}{cccc}h_0 & h_1 & \cdots & h_{n_a-1}\end{array}\right]$, intrinsically provide the solution to $F(q^{-1})$ and $H(q^{-1})$ from the diophantine Eq. (6) and Eq. (8), respectively [14].

Using the future portion relating to $\xi(k)$ and comparing it with Eq. (5), it is possible to explain $E(q^{-1})$ by moving Eq. (5) N_y steps back. Therefore, the calculation of the $E(q^{-1})$ polynomial is given by

$$E\left(q^{-1}\right)=1+\mathbf{C}\mathbf{A}^0\boldsymbol{\Gamma}q^{-1}+\mathbf{C}\mathbf{A}^1\boldsymbol{\Gamma}q^{-2}+\cdots+\mathbf{C}\mathbf{A}^{N_y-2}\boldsymbol{\Gamma}q^{-(N_y-1)}\tag{19}$$

From that same observation, using the future portion related to $u(k)$ and comparing it with Eq. (7), it is possible to obtain the filter $J(q^{-1})$ by moving Eq. (7) N_y-d steps back. The calculation of $J(q^{-1})$ is given by

$$J\left(q^{-1}\right)=\mathbf{C}\mathbf{A}^0\mathbf{B}+\mathbf{C}\mathbf{A}^1\mathbf{B}q^{-1}+\mathbf{C}\mathbf{A}^2\mathbf{B}q^{-2}+\cdots+\mathbf{C}\mathbf{A}^{N_y-d-1}\mathbf{B}q^{-(N_y-d-1)}\tag{20}$$

Therefore, from the minimization of Eq. (3), now using Eq. (18), the minimum order UHPC control law becomes

$$u\left(k\right)=\frac{y_r\left(k+d\right)-\left(\mathbf{C}\mathbf{A}^{N_y}-\mathbf{C}\mathbf{F}\mathbf{C}\right)\bar{x}\left(k\right)-\mathbf{C}\mathbf{F}y\left(k\right)}{\lambda+\mathbf{C}\mathbf{H}+\sum_{i=1}^{d-1}\mathbf{C}\mathbf{A}^{N_y-i}\mathbf{B}q^{-(d-i)}}\tag{21}$$

In [14] it was proposed the equivalence between polynomial and state space methods to design the UHPC controller. Therefore, the control law equations (12) and (21) and the MVP ones in (11) and (18) are supposedly to be equivalent as well. In this work the GMVSS method is used to find the $E(q^{-1})$, $F(q^{-1})$, $J(q^{-1})$ and $H(q^{-1})$ polynomials necessary to implement the UHPC control law in the canonical RST controller form presented in Eq. (12). In summary, the design of the UHPC controller is performed via state space to solve the two necessary Diophantine equations, speeding up the design stage, while the synthesized control law is applied via the transfer function. Furthermore, according to [23] such decision avoids the increase in the computational load associated with the implementation of the control law in the state space form.

Finally, it is important to note that using the design method presented, the problem of solving the Diophantine equations of noise and command no longer exists, making it possible to implement highly-extended prediction horizons without overloading the memory of the digital controller; UHPC's ability to deal with noise is inherited from the Kalman filter [14].

4 Performance and robustness analysis

The block diagram in the RST form of a closed-loop system is shown in Fig. 1, where the reference, output and control filters can be observed. This structure adds interesting properties to the controller to guarantee, for instance, offset-free behavior. This control representation can provide consistency to the theoretical aspects in terms of the transfer function, allowing the control loop to be assessed through classical methods established in the process control literature for robustness analysis, stability and performance [27].

A large number of control laws can be written in a generic way, known as the (canonical) RST form of controller, given by

$$R\left(q^{-1}\right)u\left(k\right)=T\left(q^{-1}\right)y_r\left(k\right)-S\left(q^{-1}\right)y\left(k\right)\tag{22}$$

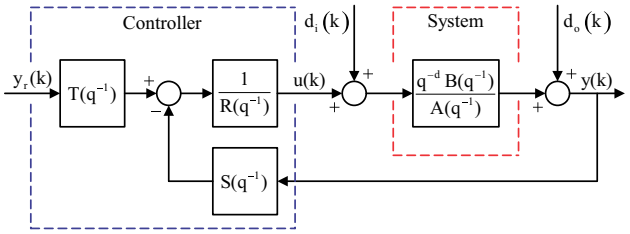

Fig. 1 Block diagram of the RST digital controller canonical form

where $R(q^{-1})$, $S(q^{-1})$ and $T(q^{-1})$ are weighting polynomials (filters) of the control signal, system output and reference signal, respectively. The controller RST format has two degrees of freedom, since the control law consists of a feedback portion $S\left(q^{-1}\right)/R\left(q^{-1}\right)$ and a feedforward portion $T\left(q^{-1}\right)/R\left(q^{-1}\right)$. The proper selection of these polynomials allows to solve both the regulation problem and the reference tracking problem in a control loop [28,29].

According to [27,28] there are two ways to consider the RST control structure: positional RST and incremental RST. The positional RST structure is represented by Eq. (22) and does not guarantee reference tracking and disturbance rejection for systems without integrators, while the incremental RST does. The incremental RST structure is given by

$$R\left(q^{-1}\right)\Delta u\left(k\right) = T\left(q^{-1}\right)y_r\left(k\right) - S\left(q^{-1}\right)y\left(k\right) \tag{23}$$

Now, in Fig. 1, considering the disturbances $d_i(k)$ and $d_o(k)$ zero, the closed-loop transfer function is

$$T_{cl}\left(q^{-1}\right) = \frac{y\left(k\right)}{y_r\left(k\right)} = \frac{q^{-d}B\left(q^{-1}\right)T\left(q^{-1}\right)}{A\left(q^{-1}\right)R\left(q^{-1}\right) + B\left(q^{-1}\right)S\left(q^{-1}\right)} \tag{24}$$

Considering $y_r(k)$ and $d_o(k)$ zero, the closed-loop transfer function of the input disturbance $d_i(k)$ to the output of the plant $y(k)$ is

$$S_i\left(q^{-1}\right) = \frac{y\left(k\right)}{d_i\left(k\right)} = \frac{q^{-d}B\left(q^{-1}\right)R\left(q^{-1}\right)}{A\left(q^{-1}\right)R\left(q^{-1}\right) + B\left(q^{-1}\right)S\left(q^{-1}\right)} \tag{25}$$

Considering $y_r(k)$ and $d_i(k)$ zero, the closed-loop transfer function of the output disturbance $d_o(k)$ to the output of the plant $y(k)$ is

$$S_o\left(q^{-1}\right) = \frac{y\left(k\right)}{d_o\left(k\right)} = \frac{A\left(q^{-1}\right)R\left(q^{-1}\right)}{A\left(q^{-1}\right)R\left(q^{-1}\right) + B\left(q^{-1}\right)S\left(q^{-1}\right)} \tag{26}$$

The UHPC controller is a linear controller and can be written in the canonical RST form. Upon inspection of Eqs. (12) and Eq. (14), it is easy to see that for the case of the minimum order UHPC, positional or incremental, the polynomials $R(q^{-1})$, $S(q^{-1})$ and $T(q^{-1})$ are defined as

$$\begin{aligned} R\left(q^{-1}\right) &= H\left(q^{-1}\right)E\left(q^{-1}\right) + \lambda C\left(q^{-1}\right) \\ &\quad - q^{-d}F\left(q^{-1}\right)J\left(q^{-1}\right) \\ S\left(q^{-1}\right) &= F\left(q^{-1}\right) \\ T\left(q^{-1}\right) &= C\left(q^{-1}\right) \end{aligned}$$

where the parameter λ penalizes the control action. Under steady-state conditions the UHPC controller in the RST form attenuates the offset related to a measurable disturbance in a constant form and also provides time-delay compensation.

4.1 Sensitivity functions

According to [30], the robustness of a control system is analyzed from the gain margin (GM) and phase margin (PM) of the complementary sensitivity function and the sensitivity function, Eqs. (24) and (26), respectively. The sensitivity functions allow access to the closed-loop frequency response characteristics and how sensitive the control system is to changes in the plant, providing relevant information regarding the stability and robustness of the control system. The maximum amplitude ratios of the sensitivity and complementary sensitivity functions provide useful measures on the robustness of the control loop. These measures are also used as a design criterion for control systems [31].

Let $\left\|S_o\left(\mathrm{e}^{-j\omega T_s}\right)\right\|$ and $\left\|T_{cl}\left(\mathrm{e}^{-j\omega T_s}\right)\right\|$ denote the amplitude ratios of $S_o(q^{-1})$ and $T_{cl}(q^{-1})$, respectively. M_S is defined as the maximum value of $\left\|S_o\left(\mathrm{e}^{-j\omega T_s}\right)\right\|$ for all frequencies:

$$M_S = \max_{0\le\omega\le\infty}\left\|S_o\left(\mathrm{e}^{-j\omega T_s}\right)\right\| = \left\|S_o\left(q^{-1}\right)\right\|_\infty \tag{27}$$

Using Eq. (26), the sensitivity function in Eq. (27), the amplitude ratio becomes

$$\begin{aligned} M_S &= \max_{0\le\omega\le\infty}\left\|S_o\left(\mathrm{e}^{-j\omega T_s}\right)\right\| \\ &= \left\|\frac{A\left(q^{-1}\right)R\left(q^{-1}\right)}{A\left(q^{-1}\right)R\left(q^{-1}\right) + B\left(q^{-1}\right)S\left(q^{-1}\right)}\right\|_\infty \end{aligned} \tag{28}$$

The maximum value M_S also has a geometrical interpretation. The loop gain is defined as the transfer function of the controller in series with the transfer function of the plant. Then M_S is the inverse of the shortest distance from the Nyquist plot for loop gain to the critical point $(-1, j0)$. Thus, as M_S decreases, the closed-loop system becomes more robust [30,32].

Likewise M_S value, M_T is defined as the maximum value of $\left\| T_{cl}\left(\mathrm{e}^{-j\omega T_s}\right)\right\|$ for all frequencies:

$$M_T = \max_{0\leq\omega\leq\infty} \left\| T_{cl}\left(\mathrm{e}^{-j\omega T_s}\right)\right\| = \left\| T_{cl}\left(q^{-1}\right)\right\|_\infty \tag{29}$$

Using Eq. (24), the complementary sensitivity function in Eq. (29), the amplitude ratio becomes

$$\begin{aligned} M_T &= \max_{0\leq\omega\leq\infty} \left\| T_{cl}\left(\mathrm{e}^{-j\omega T_s}\right)\right\| \\ &= \left\| \frac{q^{-d} B\left(q^{-1}\right) T\left(q^{-1}\right)}{A\left(q^{-1}\right) R\left(q^{-1}\right) + B\left(q^{-1}\right) S\left(q^{-1}\right)} \right\|_\infty \end{aligned} \tag{30}$$

In a SISO sense, for achieving the desired reference tracking and disturbance rejection to the control system, at low frequencies, $M_T \rightarrow 1$ and $M_S \rightarrow 0$ and at high frequencies $M_T \rightarrow 0$ and $M_S \rightarrow 1$. Ideally, $\left\| T_{cl}\left(\mathrm{e}^{-j\omega T_s}\right)\right\|$ should be kept equal to the unit for the highest possible frequency range, while $\left\| S_o\left(\mathrm{e}^{-j\omega T_s}\right)\right\|$ should be null for all frequencies. However, this ideal situation is physically impossible for control systems, so a more realistic objective is to minimize $\left\| S_o\left(\mathrm{e}^{-j\omega T_s}\right)\right\|$ by the largest possible frequency range. For a satisfactory control system $1 \leq M_T \leq 1.5$ and $1.2 \leq M_S \leq 2$ [30].

According to [33] the maximum M_S and M_T values are related to the gain and phase margins as shown:

$$GM \geq 20\log_{10}\left(\frac{M_S}{M_S - 1}\right), \quad PM \geq 2\sin^{-1}\left(\frac{1}{2M_S}\right)\left(\frac{180^\circ}{\pi}\right) \tag{31}$$

$$GM \geq 20\log_{10}\left(1 + \frac{1}{M_T}\right), \quad PM \geq 2\sin^{-1}\left(\frac{1}{2M_T}\right)\left(\frac{180^\circ}{\pi}\right) \tag{32}$$

The GM is the amount that the loop gain can be increased before reaching the stability limit, while the PM is the amount of phase lag required to reach the stability limit [34,35].

It is worth noting that such specifications may vary between different fields of application, i.e., in the field of the chemical and petrochemical industry a well-tuned controller must provide 4.6 dB $\leq GM \leq$ 12 dB and $30^\circ \leq PM \leq 45^\circ$ [30]. In turn, the control systems designed within the aviation area have more demanding specifications, commonly in the range 6 dB $\leq GM \leq$ 15 dB and $30^\circ \leq PM \leq 60^\circ$ [35]. Finally, control systems with high GM and PM values support greater parametric changes in the plant, before reaching closed-loop instability [36].

Since UHPC is a optimal linear quadratic control technique, the UHPC control law typically provides PM approximately equal to 60° and an asymptotic reference tracking, i.e., no overshoot or greatly reduced overshoot from a physically realizable control signal, where λ is the design parameter that can be used to set the settling time of the control system, which perfectly copes with the system model energy constraints, that is, the optimization is subject to the system model. In [37,38] sub-optimal solutions are presented in order to attend specific design criteria and constraints for both performance and robustness of the control loop using Laguerre functions and Mandani fuzzy systems.

In classical control theory, robustness specifications can be built into the control loop from the beginning of the controller design, providing enough gain and phase margin to neutralize the effects of system modeling errors and external disturbances that may act on he. Unmodeled high-frequency dynamics as well as parametric plant variations (low-frequency disturbances) can act to destabilize a control loop.

Therefore, it is important to design controllers that have robust stability, which is the ability to provide stability to the control loop despite modeling errors due to unmodeled high-frequency dynamics and plant parametric variations. In addition, it is necessary that the designed controllers have robust performance, which is the ability to guarantee satisfactory performance (in terms of overshoot, settling time, steady state error, etc.) even if the system may be subject to disturbances [35].

4.2 Performance indexes

Performance indexes are widely used in the control literature as a quantitative measure of the quality of the controlled system, especially in terms of reference tracking and disturbance rejection. Such indexes assist the designer in his decision on which control technique to use or which tuning should be selected for the control system [34,39].

Four performance indices were chosen, the first two are: integral squared error (ISE) and integral absolute error (IAE) calculated by

$$ISE = \sum_{k=1}^{n} e(k)^2 \tag{33}$$

$$IAE = \sum_{k=1}^{n} \|e\,(k)\| \tag{34}$$

where $e(k) = y_r(k) - y(k)$. The other two indices are: integral squared of control (ISU), used to evaluate the control effort of each controller and is calculated from the control signal $u(k)$; total variation of control (TVC), used to compute the rate of change of the control action, based on the control increment $\Delta u(k)$, calculated by

$$\mathrm{ISU} = \sum_{k=1}^{n} u(k)^2 \tag{35}$$

$$\mathrm{TVC} = \sum_{k=1}^{n} \|\Delta u\,(k)\| \tag{36}$$

where $\Delta u(k) = u(k) - u(k-1)$. This section discussed some important concepts concerning the performance and robustness from control engineering. Performance and robustness indexes are the indices used in this paper as quantitative measures of the closed-loop stability [30].

Therefore, it is important to design controllers that have robust stability, which is the ability to provide stability to the control loop, despite modeling errors due to non-modeled high-frequency dynamics and parametric variations of the plant. In addition, it is necessary that the designed controllers have robust performance, which is the ability to guarantee satisfactory performance (overshoot, settling time, steady-state error, etc.) even if the system may be subject to disturbances [35].

Therefore, it is important to design controllers that have robust stability, which is the ability to provide stability to the control loop, despite modeling errors due to non-modeled high-frequency dynamics and parametric variations of the plant. In addition, it is necessary that the designed controllers have robust performance, which is the ability to guarantee satisfactory performance (overshoot, settling time, steady-state error, etc.) even if the system may be subject to disturbances [35].

5 Simulation results

The case study presented in this paper is the application of the UHPC to control a well-known chemical plant. The CSTR process is an irreversible exothermic first order reaction, that exhibits nonlinear behavior with stable and unstable operating points. In this way, the ability of the UHPC to deal with stable and unstable dynamics can be investigated. The dynamic response varies with the operating point and has already been a case study in [40] for GPC control and in [13] for GMV control. Consider a normalized dimensionless discrete model obtained from [41] as

$$x_1(k) = x_1(k-1) - T_s x_1(k-1) + T_s D_a (1 - x_1(k-1)) \exp\left(\frac{x_2(k-1)}{1 + x_2(k-1)/\phi_a}\right)$$

$$x_2(k) = x_2(k-1) - T_s x_2(k-1)(1+\beta_a) + T_s \beta_a u(k) + T_s B_a D_a (1 - x_1(k-1)) \exp\left(\frac{x_2(k-1)}{1 + x_2(k-1)/\phi_a}\right)$$

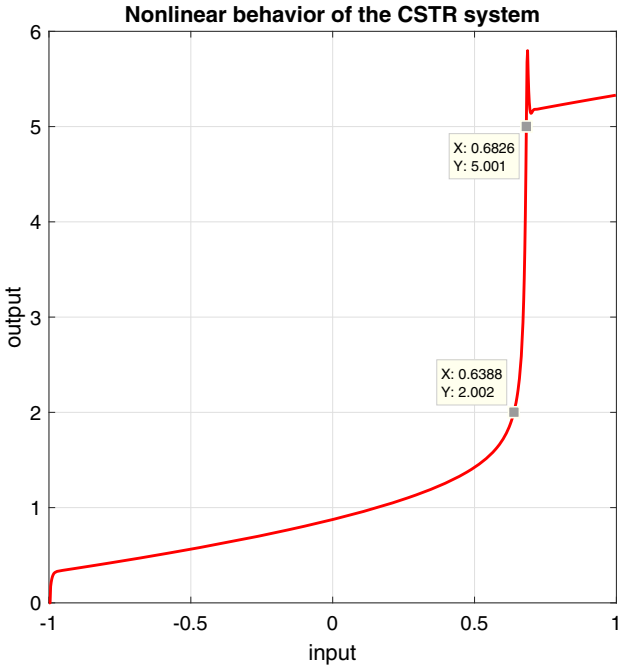

Fig. 2 Static characteristic of the CSTR

$$y(k) = x_2(k) \tag{37}$$

where $x_1(k)$ represents the dimensionless reactant concentration and $x_2(k)$ the reactor temperature. The control input, $u(k)$, is the dimensionless cooling jacket temperature. The CSTR model parameters are $D_a = 0.072$, $\phi_a = 20$, $B_a = 8$ and $\beta_a = 0.3$, meaning Damköhler number, dimensionless activation energy, heat of reaction coefficient and heat transfer coefficient, respectively.

The system in Eq. (37) exhibits numerous forms of behavior depending on the values of the physical parameters and the regions of operation. Figure 2 shows the static curve of the CSTR from the parameters given above and the major challenge is to control the system around unstable operating points, in this case, the middle temperature values.

The extended recursive least squares estimator was used to identify a second-order CARMA model. The choice of a second-order model is due to a fair comparison with previous works [13,40], where second-order models showed an adequate capture of the dynamic characteristic of the CSTR system, in addition to being a reduced-order model and thus implies a controller also of order reduced, as the UHPC is model-based. Considering the open-loop response and the characteristic curve of the CSTR system shown in n Fig. 2, the linear model was defined without time delay, so $d = 1$. A set of 1400 input and output data referring to the operating points presented in Fig. 3 was used for the estimation step and another set of 1400 data in the validation step referring to close but not equal operating points, to those of Fig. 3. The multiple correlation index R^2 is used to assess the quality of

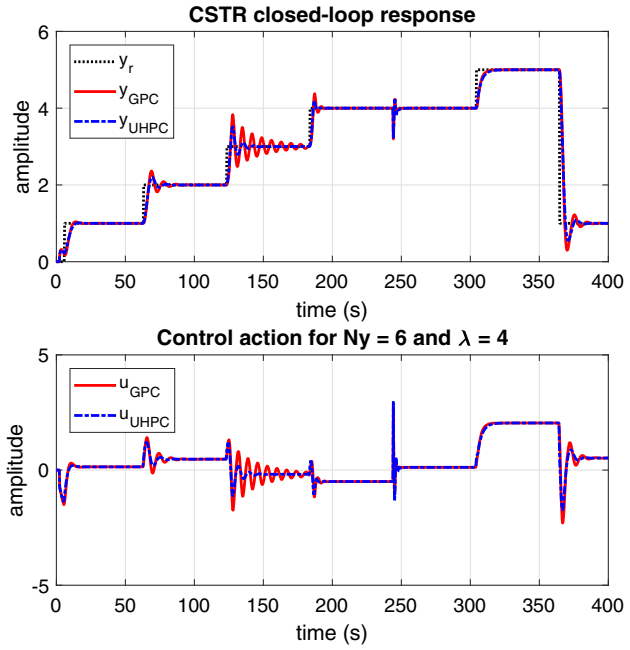

Fig. 3 Reference tracking and load disturbance rejection using GPC and UHPC

mathematical models [42] and is given by

$$R^2 = 1 - \frac{\sum_{k=1}^{N} \left[y\left(k\right) - \hat{y}\left(k\right)\right]^2}{\sum_{k=1}^{N} \left[y\left(k\right) - \bar{y}\right]^2} \tag{38}$$

where $y(k)$ is the measured output, $\hat{y}\left(k\right)$ is the model output, and $\bar{y}$ is the average of the N samples. The closer the value of R^2 is to 1, it indicates a higher quality of the evaluated model. The value of R^2 between 0.8 and 1 can be considered adequate and sufficient for many practical applications in system identification [42]. From the validation data an $R^2 = 0.9886$ was calculated for the identified model, so the model was considered quite adequate to represent the dynamics of the CSTR system. The linear model is only used to synthesize the UHPC control law that will be implemented via numerical simulation, the control signal $u(k)$ presented in Eq. (12) is applied to the nonlinear CSTR process described in Eq. (37).

Therefore, the polinomial model used for the synthesis of the controllers, for the system in Eq. (37), considering a sampling period $T_s = 0.3$ s, is given by

$$A\left(q^{-1}\right) = 1 - 1.8419q^{-1} + 0.8422q^{-2}$$
$$B\left(q^{-1}\right) = 0.0900 - 0.0888q^{-1}$$
$$C\left(q^{-1}\right) = 1 - 0.0681q^{-1} - 0.0401q^{-2}$$

The state space representation matrices of the nominal model for the system in Eq. (37) are:

$$\mathbf{A} = \begin{bmatrix} 1.8419 & 1 \\ -0.8422 & 0 \end{bmatrix} \quad \mathbf{B} = \begin{bmatrix} 0.0900 \\ -0.0888 \end{bmatrix}$$
$$\mathbf{C} = \begin{bmatrix} 1 & 0 \end{bmatrix} \quad \mathbf{\Gamma} = \begin{bmatrix} 1.7738 \\ -0.8823 \end{bmatrix}$$

The difference lies in the $C(q^{-1})$ polynomial, since for classical GPC models of the system are usually used, i.e., $C(q^{-1}) = 1$, not because it is difficult to model, but because it is difficult to handle within the GPC design for higher values of N_y, N_u. Another advantage of the UHPC is its ease of including high-order $C(q^{-1})$ by the designer, if necessary. To include the incremental action on both controllers, the CARMA model was augmented by Δ, becoming a CARIMA model, given by

$$\Delta A\left(q^{-1}\right) = 1 - 2.8419q^{-1} + 2.6841q^{-2} - 0.8422q^{-3}$$
$$B\left(q^{-1}\right) = 0.0900 - 0.0888q^{-1}$$
$$C\left(q^{-1}\right) = 1 - 0.0681q^{-1} - 0.0401q^{-2}$$

The state space representation matrices of the augmented model for the system in Eq. (37) are:

$$\mathbf{A_a} = \begin{bmatrix} 2.8419 & 1 & 0 \\ -2.6841 & 0 & 1 \\ 0.8422 & 0 & 0 \end{bmatrix} \quad \mathbf{B_a} = \begin{bmatrix} 0.0900 \\ -0.0888 \\ 0 \end{bmatrix}$$
$$\mathbf{C_a} = \begin{bmatrix} 1 & 0 & 0 \end{bmatrix} \quad \mathbf{\Gamma_a} = \begin{bmatrix} 2.7738 \\ -2.7242 \\ 0.8422 \end{bmatrix}$$

The numerical simulations in this work used the same output prediction horizon N_y and the weighting factor λ is used to fine tuning the GPC and UHPC response, in order to promote a fair comparison between the controllers. For GPC, it is assumed that the control horizon is the same as the output horizon ($N_u = N_y$).

Figures 3 and 4 show the output and control signals of the system using the classic GPC and UHPC controllers for different tunings. This case study uses reference changes around the operating range and step load disturbance $d_o(k)$ as shown in Fig. 1 (20% of the setpoint magnitude), applied at time instant 244 s. It is an interesting challenge to know if the proposed UHPC is able to control the system where the dynamics vary in different operating conditions. Both controllers are able to eliminate the load disturbance applied at the system output, as GPC and UHPC have incremental action $\Delta u(k)$.

Considering Figs. 2 and 3, it is noticed that small variations in the magnitude of the control signal $u(k)$ imply high variations in the magnitude of the output signal $y(k)$ within

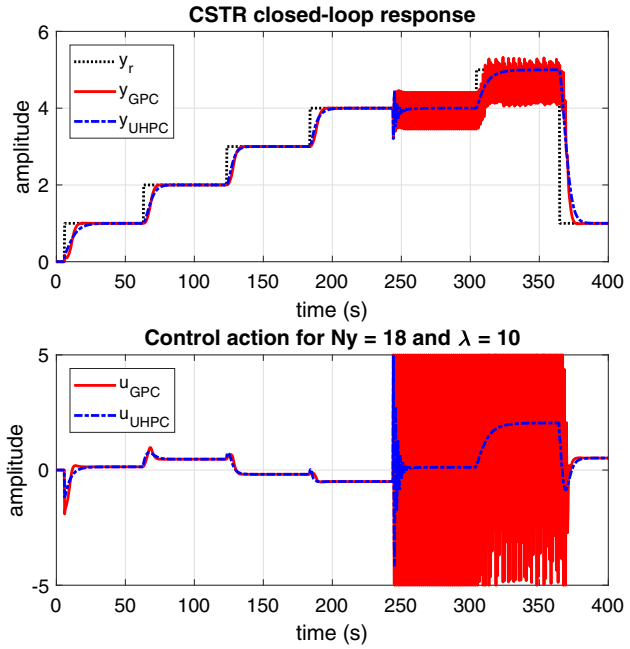

Fig. 4 Reference tracking and load disturbance rejection using GPC and UHPC

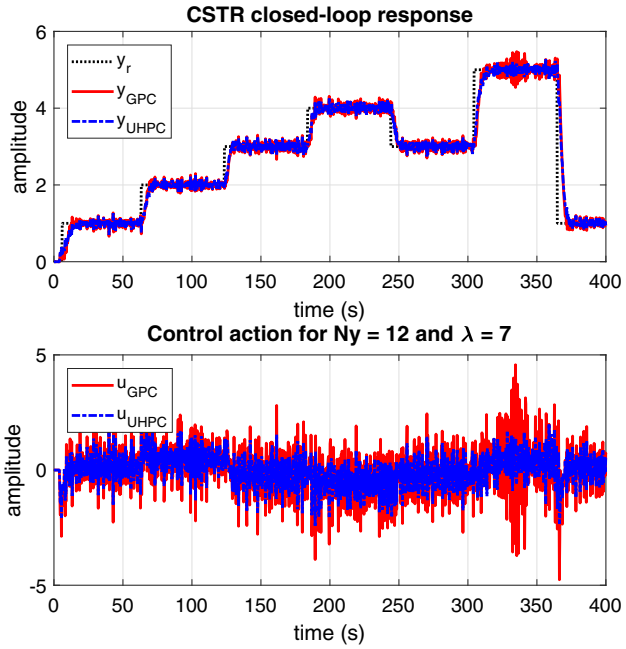

Fig. 5 Reference tracking and noise attenuation using GPC and UHPC

the operating range of 2–5, since in this region the nonlinear characteristic of the CSTR system is exacerbate. Such behavior is expected, as the UHPC and GPC control law were designed based on a linear model of the system considering a larger operating range, so the performance of both controllers is degraded for this particular operating range and even so, both the controllers are able to maintain the stability of the system thanks to their high robustness margins indicated by the GM and PM.

Also in Fig. 3, it can be observed that the GPC and UHPC controllers are able to stabilize the control loop and track the reference in all operating points even in the presence of load disturbances, however the UHPC has a more adequate performance. In Fig. 4, although the GPC and UHPC controllers present a similar reference tracking and there are no output oscillations as seen in Fig. 3 due to a tuning considering a larger N_y and λ, the GPC is unable to stabilize the control loop when the load disturbance is applied. In addition, the UHPC control effort is lower than the GPC.

Figure 5 shows the reference tracking when the system output is contaminated by a zero mean Guassian noise with variance $\sigma_\xi^2 = 0.005$. Both controllers were able to stabilize the control loop, however the GPC is more sensitive to noise and, in turn, the UHPC presents optimal noise attenuation. Table 2 shows the variances of the control increment, control signal, output signal and generalized output, $\sigma_{\Delta u}^2$, σ_u^2, σ_y^2 and σ_ϕ^2, respectively, as well as the performance indexes calculated from the temporal response shown in Fig. 5.

Table 2 Indexes and variances calculated for the CSTR system

Controller	GPC	UHPC
ISE	2.5386×10^2	1.8721×10^2
IAE	2.4513×10^2	2.0734×10^2
ISU	1.6141×10^3	6.4999×10^2
TVC	1.6224×10^3	1.0158×10^3
$\sigma_{\Delta u}^2$	2.1741×10^0	8.2690×10^{-1}
σ_u^2	1.1301×10^0	4.5500×10^{-1}
σ_y^2	1.9952×10^0	1.9696×10^0
σ_ϕ^2	1.0399×10^2	3.9386×10^1

In Fig. 6, the frequency analysis of the sensitivity functions, $T_{cl}(q^{-1})$ and $S_o(q^{-1})$, from the numerical simulation presented in Fig. 5 reveals slight differences in high frequency for the complementary sensitivity function, where the GPC controller offers greater bandwidth compared to UHPC. Observing the sensitivity function, it is noticed that for low frequencies the GPC controller offers greater rejection (attenuation) to load disturbances. Furthermore, the maximum value M_S is lower for the GPC ($M_S = 0.6928$) in relation to the UHPC ($M_S = 0.7417$). The M_S value is of paramount importance for the control loop in order to mitigate high frequency disturbances, sensor noise and to be robust to unmodeled high frequency dynamics.

Table 3 shows the maximum M_S and M_T values calculated for the controllers in each control system simulated in Figs. 3, 4 and 5. It is observed that the values of M_S decrease

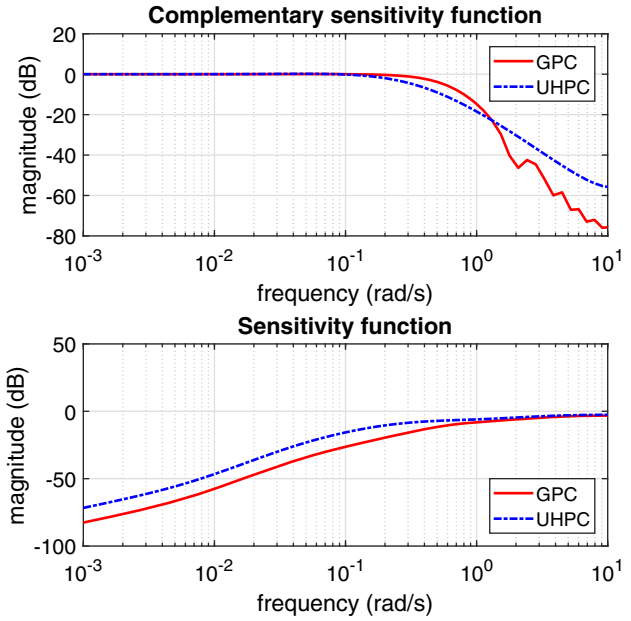

Fig. 6 Frequency response using GPC and UHPC

Table 3 Maximum values calculated for the CSTR system

Control	M_T	M_S
GPC ($N_y = 6$ and $\lambda = 4$)	1.0364	0.8039
UHPC ($N_y = 6$ and $\lambda = 4$)	1.0295	0.7928
GPC ($N_y = 18$ and $\lambda = 10$)	1.0000	0.6667
UHPC ($N_y = 18$ and $\lambda = 10$)	1.0055	0.7192
GPC ($N_y = 12$ and $\lambda = 7$)	1.0073	0.6928
UHPC ($N_y = 12$ and $\lambda = 7$)	1.0236	0.7417

as λ increases. The higher its value, the more conservative the control action becomes and, moreover, high values of λ increase the variance of $y(k)$ and decrease the variance of $u(k)$, while small values of λ produce the inverse effect.

In Fig. 7 the closed-loop response for different λ values is presented, it can be seen that for $\lambda = 25$, the system output oscillates around the reference, having difficulties to stabilize the system for such operating points. The closed-loop response for different values of N_y is shown in Fig. 8, it is observed that only for $N_y = 15$, the system output is able to adequately track the reference at all operating points of the system. In turn, the other values selected for N_y fail to provide reference tracking at the all three operating points of the CSTR system. It is worth remembering that the last two operating points belong to the intermediate range where the nonlinearity of the system is stronger, making the work of the UHPC more difficult.

Now regarding the computational load for implementing each control law in the RST form (see Fig. 1), the specifications of the computer used in simulations are: Intel® Core™

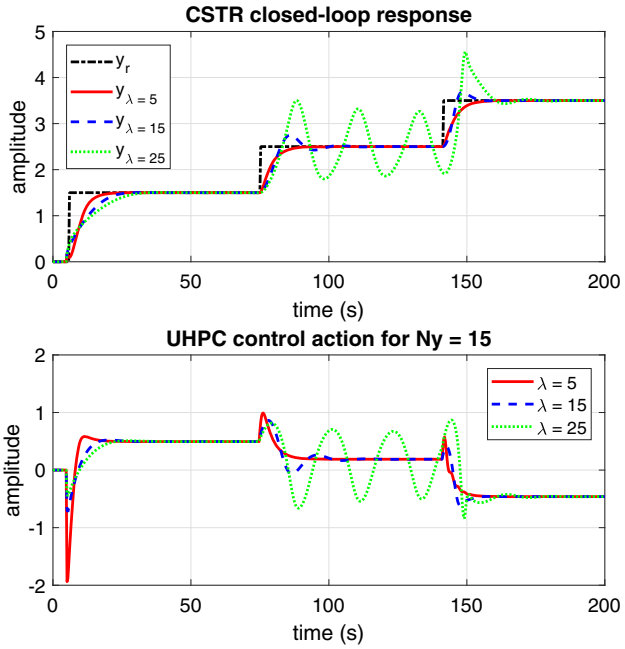

Fig. 7 Reference tracking using UHPC with fixed N_y and different λ values across three operating points

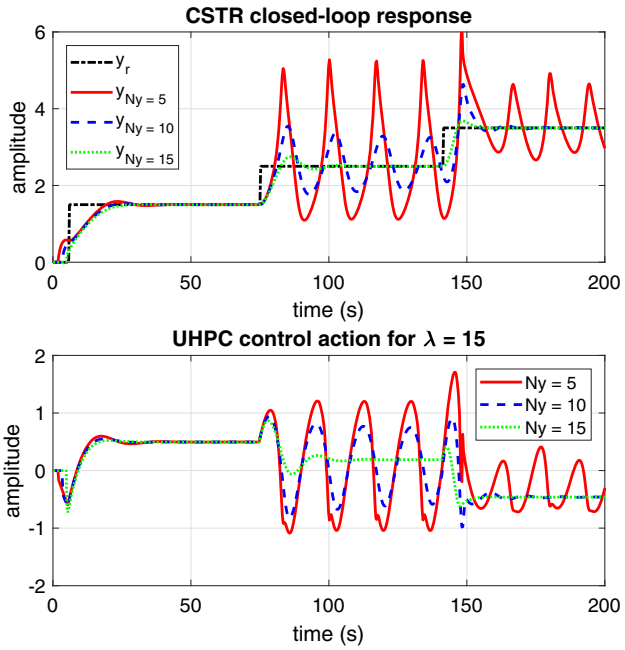

Fig. 8 Reference tracking using UHPC with fixed λ and different N_y values across three operating points

i5-8250U CPU 1.60 GHz; 8.00 GB RAM memory installed; 64bit Windows 10 Home Single Language Operating System (Version 21H1). The software used was MATLAB® 2019b. Table 4 shows the number of parameters (number of controller coefficients in RST form) and the runtime in seconds of 1 (one) iteration of the GMV, GPC and UHPC predictive controllers, in addition to the classic and widely

Table 4 Computational load for each control law

Control Law	Runtime	Parameters
UHPC	6.30×10^{-6} s	27
GPC	5.10×10^{-6} s	24
GMV	6.20×10^{-6} s	10
PID	4.10×10^{-6} s	8

disseminated, in industry and in the academic community, PID (Proportional Integral Derivative) control for the numerical simulation presented in Fig. 4. From Table 4, it can also be concluded that although the UHPC has more than triple the coefficients in its RST controller structure than the PID, this is not an obstacle for its implementation, since the runtime of the the control law of both remains extremely fast and the processing capacity of controllers or any electronic device keeps growing over the last few decades. Only the UHPC and GPC controllers were able to stabilize the control system and promote proper reference tracking at all CSTR operating points, which did not happen for the GMV and PID controllers, therefore, such controllers are not suitable candidates for the case study addressed in this work. It is worth remembering that the proposed UHPC has 2 tuning parameters (N_y and λ), while the GPC (N_y, N_u and λ) and PID (K_p, K_i and K_d) have 3 tuning parameters.

The tuning for GMV is $N_y = d = 1$ and for UHPC it is $N_y = 15$. Both controllers have the same control weighting factor $\lambda = 15$. From Fig. 9, it is clear that the GMV control is unable to stabilize the system for all operating points considered, as well as the PID control, which was unable to maintain system stability at any operating point.

Figure 10 shows the behavior of the control system when the CSTR process undergoes parametric variations in D_a, ϕ_a, B_a and β_a. At the instant of time $t = 244$ s, the 4 parameters present in Eq. (37) change to $D_a = 0.0648$, $\phi_a = 30$, $B_a = 6$ and $\beta_a = 0.5$. Both controllers can stabilize the system even in the presence of such variations, however the GPC control presents sustained oscillations and a higher energy cost. Therefore, once again, the UHPC control proves to be more robust to variations in system parameters for the same prediction horizon.

Figure 11 shows the control system when it is started with non-zero initial conditions for $x_1 = x_2 = 2$. It can be seen that the output quickly tracks the reference without any complications. Once again, it can be seen that the UHPC is able to provide greater damping with less control effort than the GPC for the same prediction horizon.

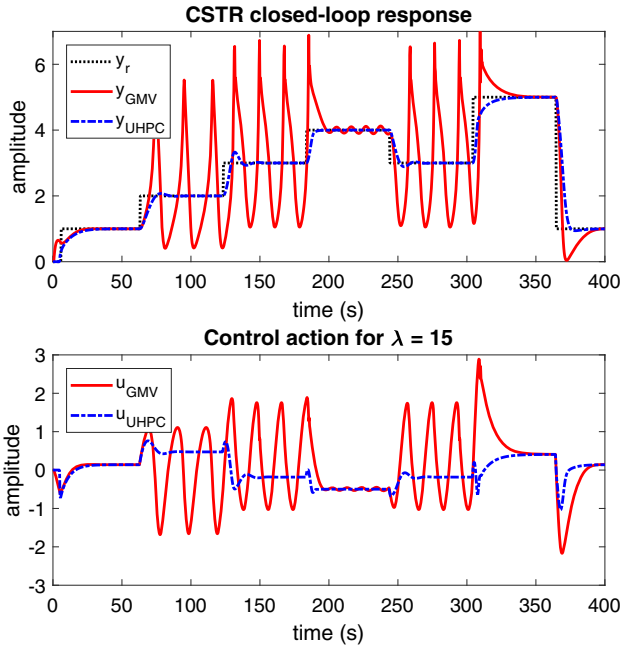

Fig. 9 Reference tracking using UHPC and GMV with fixed λ value across five operating points

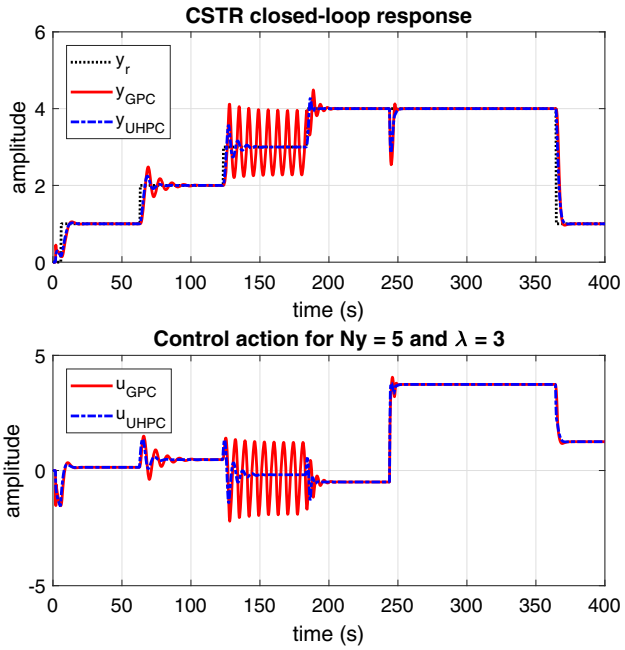

Fig. 10 Reference tracking using UHPC and GPC in the presence of parametric variations

6 Conclusions

In this paper, the minimum order UHPC design applied to a CSTR nonlinear system found in the chemical area was presented. The numerical results of the UHPC are compared to the classic GPC and GMV with regard to the stability, performance and robustness of the control loop. GMV and

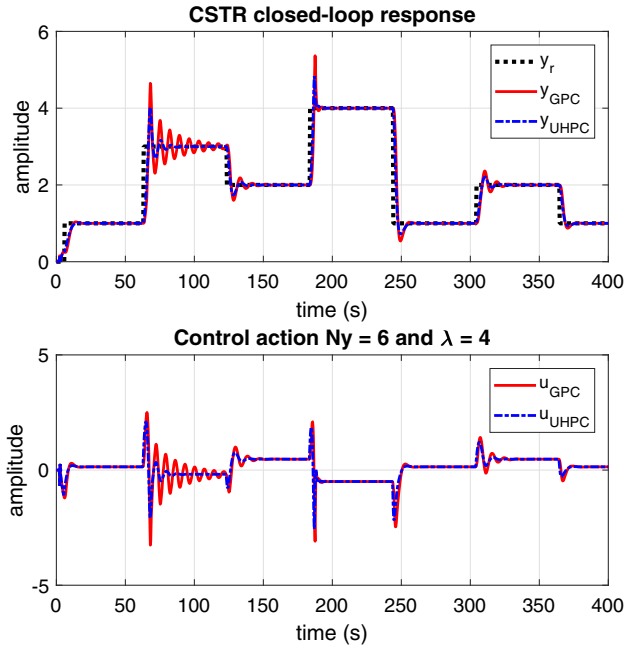

Fig. 11 Reference tracking using UHPC and GPC for non-zero initial conditions

GPC are a members of the predictive controller family, well known in academia and industry.

There are two main differences between these two control methods: the UHPC is based on the CARMA model and the GPC is usually based on the CAR model, which improves the UHPC's ability to regulate the system output even in the presence of modeling errors, external disturbances and noise measurement; the UHPC control law has approximately the same computational cost to implement in relation to the GPC control law, however, UHPC is capable of providing smaller variances in the signals of interest to the control system when compared to GPC.

The case study was evaluated in a CSTR system. It has a nonlinear behavior with stable and unstable operating points and different static gains depending on the operating point. The goal was to show that the UHPC controller is efficient to handle steady-state error even on different system dynamics and load disturbance applied to the system output. The UHPC has a more uniform response compared to the GPC for the system's operating range, which indicates greater robustness despite the dynamic changes. The temporal responses and the calculated performance indexes confirmed that the UHPC was able to provide greater stability margins than the GPC. Another important characteristic of UHPC in relation to GPC was the ability to reduce all variances of interest when the system's output was contaminated with noise. The UHPC control signal was less sensitive to noise than the GPC. It was also observed a greater robustness of the UHPC in maintaining the stability of the CSTR process even in the presence of parametric variations when compared to the GPC.

Finally, the UHPC was more suitable than the GPC to control the studied CSTR system, where it is concluded that it is an excellent candidate to be applied in system classes where others predictive controllers present satisfactory performance or in systems with complex dynamics.

Acknowledgements The first author would like to acknowledge the financial support provided by the Brazilian Foundation: Coordination for the Improvement of Higher Education Personnel (CAPES).

Author Contributions Luís A. M. de Castro: Conceptualization; Methodology; Software; Writing – Original Draft. Antonio da S. Silveira: Resources; Writing – Review & Editing; Supervision. Rejane de B. Araújo: Validation, Data Curation; Writing – Review & Editing.

Funding The authors thankfully acknowledge the financial support of the Brazilian Coordination for the Improvement of Higher Education Personnel (CAPES) through the Social Demand Program (Doctoral level).

Declarations

Conflict of interest The authors declare that they have no conflict of interest.

References

1. Wang L (2009) Model predictive control system design and implementation using MATLAB®. Springer, Berlin
2. Åström KJ (1970) Introduction to stochastic control theory. Academic Press, New York
3. Clarke DW, Gawthrop PJ (1975) Self-tuning controller. Proc Inst Electr Eng 122(9):929–934. https://doi.org/10.1049/piee.1975.0252
4. Clarke DW, Mohtadi C, Tuffs PS (1987a) Generalized predictive control—Part I: the basic algorithm. Automatica. https://doi.org/10.1016/0005-1098(87)90087-2
5. Camacho EF, Bordons C (2007) Model predictive control, 2nd edn. Springer, London
6. Cutler CR, Ramaker BL (1980) Joint Automatic Control Conference, San Francisco, USA, vol 17, p 72
7. Clarke DW, Mohtadi C (1989) Properties of generalized predictive control. Automatica 25(6):859–875. https://doi.org/10.1016/0005-1098(89)90053-8
8. Åström KJ, Wittenmark B (2011) Computer-controlled systems: theory and design, 3rd edn. Dover, Mineola
9. Dorf RC, Bishop RH (2011) Modern control systems, 12th edn. Pearson, Upper Saddle River
10. Rossiter JA (2004) Model-based predictive control: a practical approach. CRC Press, London
11. Clarke DW, Mohtadi C, Tuffs PS (1987b) Generalized predictive control—part II: extensions and interpretations. Automatica. https://doi.org/10.1016/0005-1098(87)90088-4
12. Trentini R, Silveira A, Bartsch MT, Kutzner R, Hofmann L (2016b) In 2016 UKACC 11th International Conference on Control (CONTROL), Belfast, UK. (IEEE), pp. 1–6. https://doi.org/10.1109/CONTROL.2016.7737552

13. Coelho AAR, Araújo RB, Silveira AS (2014) Steady state tracking properties for the generalized minimum variance controller: a review, proportional integral derivative tuning and applications. Ind Eng Chem Res 53(4):1470–1477. https://doi.org/10.1021/ie400900q
14. Trentini R, Silveira A, Kutzner R, Hofmann L (2016a) In 2016 European Control Conference (ECC) (IEEE), Aalborg, Denmark, pp 1322–1327. https://doi.org/10.1109/ECC.2016.7810472
15. de Lima Jr JC, Trentini R, Prioste F (2020) Comparative study of the pitch control of a wind turbine using linear quadratic gaussian and the unrestricted horizon predictive controller. Int Trans Electr Energy Syst. https://doi.org/10.1002/2050-7038.12720
16. Silveira AS, Coelho AA (2011) Generalised minimum variance control state-space design. IET Control Theory Appl 5(15):1709–1715. https://doi.org/10.1049/iet-cta.2011.0099
17. Grimble MJ, Pang Y (2007) In 2007 46th IEEE conference on decision and control (IEEE), pp 1628–1633. https://doi.org/10.1109/CDC.2007.4434359
18. Grimble MJ (2011) Nonlinear minimum variance state space based estimation for discrete time multi channel systems. IET Signal Proc 5(4):365–378. https://doi.org/10.1049/iet-spr.2009.0064
19. Silveira A, Trentini R, Coelho A, Kutzner R, Hofmann L (2016) Generalized minimum variance control under long-range prediction horizon setups. ISA Trans 62:325–332. https://doi.org/10.1016/j.isatra.2016.01.019
20. Gallego AJ, Sánchez AJ, Berenguel M, Camacho EF (2020) Adaptive ukf-based model predictive control of a fresnel collector field. J Process Control 85:76–90. https://doi.org/10.1016/j.jprocont.2019.09.003
21. Xie S, Xie Y, Ying H, Jiang Z, Gui W (2019) Neurofuzzy-based plant-wide hierarchical coordinating optimization and control: An application to zinc hydrometallurgy plant. IEEE Trans Industr Electron 67(3):2207–2219. https://doi.org/10.1109/TIE.2019.2902790
22. Nascimento TP, Basso GF, Dórea CE, Gonçalves LMG (2019) Perception-driven motion control based on stochastic nonlinear model predictive controllers. IEEE/ASME Trans Mechatron 24(4):1751–1762. https://doi.org/10.1109/TMECH.2019.2916562
23. Silveira A, Silva A, Coelho A, Real J, Silva O (2020) Design and real-time implementation of a wireless autopilot using multivariable predictive generalized minimum variance control in the state-space. Aerosp Sci Technol 105:106,053. https://doi.org/10.1016/j.ast.2020.106053
24. Fang J, Ma R, Deng Y (2020) Identification of the optimal control strategies for the energy-efficient ventilation under the model predictive control. Sustain Cities Soc 53:101,908. https://doi.org/10.1016/j.scs.2019.101908
25. Lewis FL, Xie L, Popa D (2017) Optimal and robust estimation: with an introduction to stochastic control theory. CRC Press, London
26. Li Z, Evans RJ, Wittenmark B (1997) Minimum variance prediction for linear time-varying systems. Automatica 33(4):607–618. https://doi.org/10.1016/S0005-1098(96)00210-5
27. Landau ID, Zito G (2006) Digital control systems: design, identification and implementation. Springer, London
28. Åström KJ, Wittenmark B (2008) Adaptive control, 2nd edn. Dover, Mineola
29. Cunha LB, Castro LAM, Silveira AS, Júnior WB (2019) Digital control design by the polynomial method with evaluation of the sensitivity function. Anais da Sociedade Brasileira de Automática 1(1). https://doi.org/10.20906/CPS/CBA2018-0285
30. Seborg DE, Mellichamp DA, Edgar TF, Doyle FJ III (2010) Process dynamics and control, 3rd edn. Wiley, New Jersey
31. Doyle JC, Francis BA, Tannenbaum AR (1990) Feedback control theory. Macmillan, New York
32. Åström KJ, Hägglund T, Controllers PID (1995) Theory, design, and tuning, 2nd edn. Instrument Society of America, New York
33. Skogestad S, Postlethwaite I (2005) Multivariable feedback control: analysis and design, 2nd edn. Wiley, New York
34. Skogestad S (2003) Simple analytic rules for model reduction and PID controller tuning. J Process Control 13(4):291–309. https://doi.org/10.1016/S0959-1524(02)00062-8
35. Stevens BL, Lewis FL, Johnson EN (2016) Aircraft control and simulation: dynamics, controls design, and autonomous systems. Wiley, New Jersey
36. Fadali MS, Visioli A (2013) Digital control engineering: analysis and design, 2nd edn. Academic Press, Oxford
37. Pinheiro TCF, Silveira AS (2021) Constrained discrete model predictive control of an arm-manipulator using Laguerre function. Optim Control Appl Methods 42(1):160–179. https://doi.org/10.1002/oca.2667
38. Silveira AS, Rodríguez JE, Coelho AA (2012) Robust design of a 2-dof gmv controller: a direct self-tuning and fuzzy scheduling approach. ISA Trans 51(1):13–21. https://doi.org/10.1016/j.isatra.2011.07.006
39. Vilanova R, Visioli A (2012) PID control in the third millennium: lessons learned and new approaches. Springer, London
40. Araújo RB, Coelho AAR (2017) Filtered predictive control design using multi-objective optimization based on genetic algorithm for handling offset in chemical processes. Chem Eng Res Des 117:265–273. https://doi.org/10.1016/j.cherd.2016.10.038
41. Hernandez E, Arkun Y (1993) Control of nonlinear systems using polynomial Arma models. AIChE J 39(3):446–460. https://doi.org/10.1002/aic.690390308
42. Brosilow C, Joseph B (2002) Techniques of model-based control. Prentice Hall, Prentice